

- Chem. Soc.*, **99**, 1916 (1977).
- (23) R. Destro, T. Pilati, and M. Simonetta, *J. Am. Chem. Soc.*, **100**, 6507 (1978). We thank Professor Simonetta for communicating these results prior to publication.
- (24) In our earlier study²² we were primarily concerned with the central bond length of **8**, and in this respect the EFF prediction is in excellent agreement with experiment (calcd²² 1.595 Å; found²³ 1.606 Å).
- (25) See ref 22 for a definition of ϕ_r and ϕ_c .
- (26) To demonstrate that a significant energy barrier separates **8a** and **8c**, the values of ϕ_r and ϕ_c for each form were transformed in a direction toward the corresponding values for the other minimum. Upon relaxation, these two new structures returned to the minima from which they were derived. This procedure did modify the structure of **8** slightly from that reported in ref 22.
- (27) We have noticed this phenomenon in other cases. For example, an extensive search²⁸ of the hyperspace of gauche **5** has uncovered seven gauche minima, four more than previously^{20b} reported. (However, all new gauche minima were more than 5 kcal/mol higher in energy than the anti ground state.)
- (28) D. A. Dougherty, Ph.D. Thesis, Princeton University, 1978.
- (29) E. M. Engler, J. D. Andose, and P. v. R. Schleyer, *J. Am. Chem. Soc.*, **95**, 8005 (1973).
- (30) Although *cis*- and *trans*-decalin are not conformational isomers, we include them here since they are constitutionally identical.
- (31) We note that for these and all other compounds studied here for which the data are available, the EFF-EHMO energies are significantly (5–15 eV) lower than the previously reported^{5a} EH energies. This result is perhaps not surprising since standard geometries were used in the earlier study.^{5a}
- (32) D. N. J. White and M. J. Bovill, *J. Chem. Soc., Perkin Trans. 2*, 1610 (1977); N. L. Allinger, *J. Am. Chem. Soc.*, **99**, 8127 (1977).
- (33) S. G. Baxter, H. Fritz, G. Hellmann, B. Kitschke, H. J. Lindner, K. Mislow, C. Rüchardt, and S. Weiner, submitted for publication.
- (34) H.-D. Beckhaus, G. Hellmann, C. Rüchardt, B. Kitschke, and H. J. Lindner, *Chem. Ber.*, **111**, 3780 (1978).
- (35) D. A. Dougherty, K. Mislow, J. W. Huffman, and J. Jacobus, *J. Org. Chem.*, in press.
- (36) P. George, M. Trachtman, C. W. Bock, and A. M. Brett, *Tetrahedron*, **32**, 317 (1976).
- (37) EH energies refer to hypothetical motionless molecules at 0 K, and, in keeping with general practice, we assume that contributions by the vibrational zero-point energy, and by thermal energies of translation, rotation, and vibration, are additive and thus of little importance for relative conformer energies and quantities derived from homodesmotic reactions.
- (38) The following EFF-EHMO energies (eV) are required for homodesmotic reactions using the ALL 71 (or EAS) EFF; ethane, -248.1214 (-248.0490); propane, -353.9602 (-353.8723); isobutane, -459.7384 (-459.6363); neopentane, -565.4519 (-565.3359).
- (39) Alternatively, the strain energy of a molecule may be considered to equal $-\Delta H$ for the appropriate homodesmotic reaction. This approach leads to essentially the same results using the EFF-EHMO method, except that the strain energies are generally several kilocalories per mole smaller.
- (40) T. Clark, T. McO. Knox, H. Mackle, and M. A. McKervey, *J. Chem. Soc., Chem. Commun.*, 666 (1975).

Excited-State Spectroscopy of Hexacyanocobaltate(III)

L. Viaene,^{1a} J. D'Olieslager,^{*1a} A. Ceulemans,^{1b} and L. G. Vanquickenborne^{*1b}

Contribution from the Department of Chemistry, University of Leuven, Celestijnenlaan 200F, B-3030 Heverlee, Belgium. Received August 15, 1978

Abstract: The hexacyanocobaltate(III) anion, dissolved in an EPA matrix at 94 K, gives rise to a well-structured transient spectrum in the 365–500-nm range. By means of a straightforward ligand field analysis the observed absorbance could be identified as the absorption spectrum of an excited ${}^3T_{1g}$ state of the complex. Transitions to several components of a triplet cluster, arising from a $(t_{2g})^4(e_g)^2$ configuration, were assigned. The interpretation is shown to be consistent with the luminescence properties of this species. The present data allow for a direct electronic characterization of a relaxed excited state. The relevance of our results to the photochemistry of trivalent cobaltum compounds is discussed.

Introduction

The absorption spectrum of an excited state offers an unusual, but quite instructive, view of the energy level pattern of a given molecule. A number of other excited states, that are otherwise inaccessible from the ground state (due to selection rules, for instance), may now become observable. In some cases, the excited state relaxes into a metastable species, characterized by a novel geometrical structure. Obviously, the excited-state spectrum constitutes one of the major keys in elucidating this structure; moreover, it can be expected to contribute significantly to the understanding of the photo-physics and the photochemistry of the molecule under consideration.

In transition-metal chemistry, only a very limited number of transient spectra have been observed;² so far, especially Cr(III) complexes have been studied.^{3–6} Indeed, it has been found that these d^3 systems can be further excited from their lowest excited doublet states. As these doublet states belong essentially to the same t_{2g}^3 electronic configuration as the quartet ground state, one does not anticipate a large change in geometry. The spectral assignments are still controversial.

Virtually no data are available at present for the important class of d^6 complexes (Co(III), Rh(III), Ru(II), Fe(II)), except for a report on $[\text{Ru}(\text{bpy})_3]^{2+}$, where a triplet charge transfer state is supposed to give rise to a triplet-triplet absorption

peak,⁷ and for a preliminary communication by Adamson and co-workers⁸ on $\text{Rh}(\text{NH}_3)_5\text{Cl}^{2+}$.

In this note, we present the excited state absorption spectrum of hexacyanocobaltate(III), measured at low temperature in a glass matrix. We suggest a straightforward identification of the observed bands in the framework of a ligand field model.

Experimental Section

A 3×10^{-2} M solution of $[(\text{C}_4\text{H}_9)_4\text{N}]_3\text{Co}(\text{CN})_6$ in EPA was prepared in the dark and pipetted into a quartz $1 \times 1 \times 4$ cm spectrophotometer cell. The cell was suspended in an all-quartz Dewar, equipped with three sets of flat windows. The sample was cooled by means of a stream of cold nitrogen gas.

The excitation system consisted of a 2000 JK Lasers Ltd. Q switched ruby laser with frequency doubler. The system has an output at 347 nm of 270 mJ in 30 ns. The beam cross section is 4×8 mm.

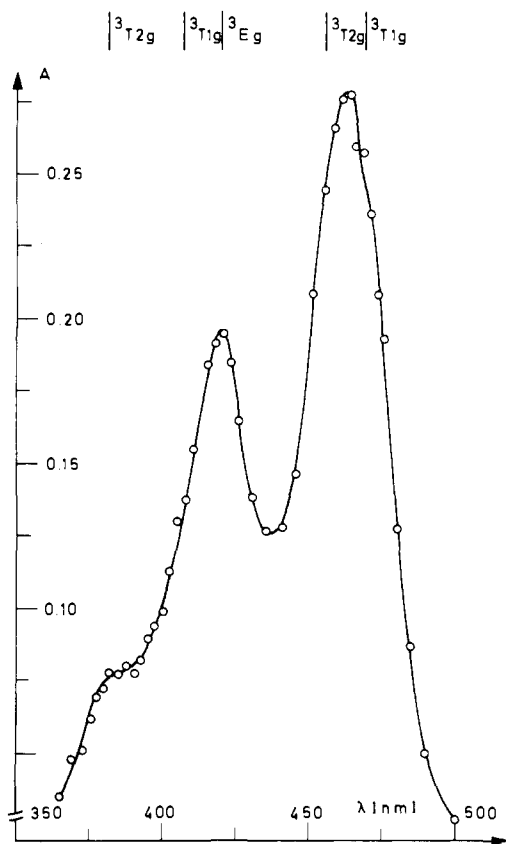
A 250-W stabilized xenon arc was used as the source of the detection light. It was passed through the sample at an angle of 90° with respect to the direction of excitation. The cross section of the detection beam was limited so as to probe only the volume contained in the first 1 mm irradiated by the exciting light. Since the laser light was appreciably absorbed by the sample, this volume contained the largest concentration of excited species.

Absorbance changes were detected through a Jobin Yvon HD 20 monochromator by means of a 1P28A photomultiplier and a type 476 Tektronix oscilloscope.

The present data were recorded at a temperature of 94 K. Ab-

Table I. Strong Field Energy Expressions for a Number of d^6 States as a Function of the Crystal Field Parameters from Reference 17

t^6	${}^1A_{1g}$	$15A - 30B + 15C$		
t^5e	${}^3T_{1g}$	$15A - 30B + 12C + 10Dq$		
t^4e^2	3A_2	$15A - 16B + 14C + 20Dq$		
	3E	$15A - 25B + 11C + 20Dq$		
	3T_2	$t_2^4({}^3T_1)e^2({}^3A_2)$	$t_2^4({}^3T_1)e^2({}^1E)$	
		$15A - 27B + 11C + 20Dq$	$\frac{2B\sqrt{2}}{2B\sqrt{2}}$	
		$2B\sqrt{2}$	$15A - 23B + 11C + 20Dq$	
	3T_1	$t_2^4({}^3T_1)e^2({}^1A_1)$	$t_2^4({}^3T_1)e^2({}^1E)$	$t_2^4({}^1T_2)e^2({}^3A_2)$
		$15A - 15B + 13C + 20Dq$	$-10B$	0
		$-10B$	$15A - 23B + 11C + 20Dq$	$2B\sqrt{3}$
		0	$2B\sqrt{3}$	$15A - 25B + 11C + 20Dq$
	5T_2	$15A - 35B + 7C + 20Dq$		

**Figure 1.** Absorption spectrum of the transient obtained from $\text{Co}(\text{CN})_6^{3-}$ immediately after laser excitation ($T = 94 \text{ K}$). The calculated levels are indicated on top of the figure.

sorbance changes were monitored from 500 to 365 nm. In this spectral region $[(\text{C}_4\text{H}_9)_4\text{N}]_3\text{Co}(\text{CN})_6$ shows no ground-state absorption.

In Figure 1 the absorbance observed immediately after the laser pulse is plotted as a function of wavelength. Absorption maxima are observed at 462 ($2.16 \mu\text{m}^{-1}$) and 419 nm ($2.38 \mu\text{m}^{-1}$) and a shoulder at about 385 nm ($2.6 \mu\text{m}^{-1}$). Below 365 nm the transient absorption signals are partially masked by the onset of the first ligand field band of $\text{Co}(\text{CN})_6^{3-}$. The absorbing species disappears in a first-order reaction with a rate constant of $4.4 (\pm 0.4) \times 10^4 \text{ s}^{-1}$. Within the limits of detection the original amount of $[(\text{C}_4\text{H}_9)_4\text{N}]_3\text{Co}(\text{CN})_6$ is restored.

Nature of the Intermediate

It is almost certain that the observed intermediate is *not* a reaction intermediate such as $\text{Co}(\text{CN})_5^{2-}$, and this for two reasons.

(1) $\text{Co}(\text{CN})_5(\text{C}_2\text{H}_5\text{OH})^{2-}$, measured in exactly the same circumstances, does not produce the transient spectrum in the 365–500-nm range. Yet one would expect that the weakness of the Co–ethanol bond should be responsible for an even easier

production of precisely the same fragment.

(2) The intermediate reacts back to form $\text{Co}(\text{CN})_6^{3-}$ in its ground state. Indeed, after the decay, an unchanged quantity of $\text{Co}(\text{CN})_6^{3-}$ is found back in the sample. If $\text{Co}(\text{CN})_5^{2-}$ were formed, one would expect it to react with the solvent to form the substitution product $\text{Co}(\text{CN})_5(\text{C}_2\text{H}_5\text{OH})^{2-}$. Actually, this product is only detected to a significant extent at much higher temperatures.

Therefore, it appears quite reasonable to assume that the transient is simply an excited state of $\text{Co}(\text{CN})_6^{3-}$ itself. It is well-known that crystalline $\text{K}_3\text{Co}(\text{CN})_6$ at low temperatures exhibits a very typical phosphorescence from a fairly long-lived level.⁹ According to Hipps and Crosby,¹⁰ this phosphorescent level corresponds to the ${}^3T_{1g}$ triplet state—the same state which is also supposed to be the precursor (at higher temperatures) of a number of photochemical substitution reactions.^{11,12} We suggest that this excited ${}^3T_{1g}$ state is also the transient from where the absorptions of Figure 1 are taking place.

Assuming a unit efficiency for the population of the triplet state, the molar extinction coefficient at 462 nm was calculated to be about $500 \text{ M}^{-1} \text{ cm}^{-1}$, which is suggestive of d–d bands. In the next section, the ${}^3T_{1g}$ hypothesis will be examined in the framework of ligand field theory.

Ligand Field Analysis

1. Ground-State Spectrum. The $\text{Co}(\text{CN})_6^{3-}$ complex exhibits two prominent ligand field bands with a rather obvious assignment: the ${}^1A_{1g} \rightarrow {}^1T_{1g}$ transition is at $\sim 3.25 \mu\text{m}^{-1}$ (308 nm), while the ${}^1A_{1g} \rightarrow {}^1T_{2g}$ transition is at $\sim 3.92 \mu\text{m}^{-1}$ (256 nm).¹³ The weak shoulder^{14–16} at $\sim 2.52 \mu\text{m}^{-1}$ (396 nm) is assigned as the ${}^1A_{1g} \rightarrow {}^3T_{1g}$ transition. The first-order energy expressions are given by

$$\begin{aligned} {}^3A_{1g} \rightarrow {}^3T_{1g} & 10Dq - 3C \\ {}^1T_{1g} & 10Dq - C \\ {}^1T_{2g} & 10Dq - C + 16B \end{aligned}$$

Accounting for configuration interaction within the ligand field manifold, one obtains $10Dq = 3.52 \mu\text{m}^{-1}$, $B = 0.0448 \mu\text{m}^{-1}$, $C = 0.3548 \mu\text{m}^{-1}$. Figure 2 shows the three relevant configurations (A) and the corresponding state energies (B), calculated with the here-obtained parameter set. From the present point of view, the $t_{2g}^4e_g^2$ configuration is especially important, since it might become observable in ${}^3T_{1g}(t^5e^1)$ excited state absorption. As shown in Figure 2B, the $t_{2g}^4e_g^2$ configuration gives rise to one rather low-lying quintet ${}^5T_{2g}$ at $4.1 \mu\text{m}^{-1}$, a cluster of five triplet states around $6 \mu\text{m}^{-1}$, two more or less isolated triplets at $\sim 7.3 \mu\text{m}^{-1}$, and several singlets (only the least energetic ${}^1T_{2g}$ at $6.5 \mu\text{m}^{-1}$ has been included). The relevant parametric energy expressions are given in Table I.

Since $C \gg B$, the C parameter will be the dominant factor in determining the differential interelectronic repulsion. Table I shows that the five triplets in the first cluster (of $t_{2g}^4e_g^2$

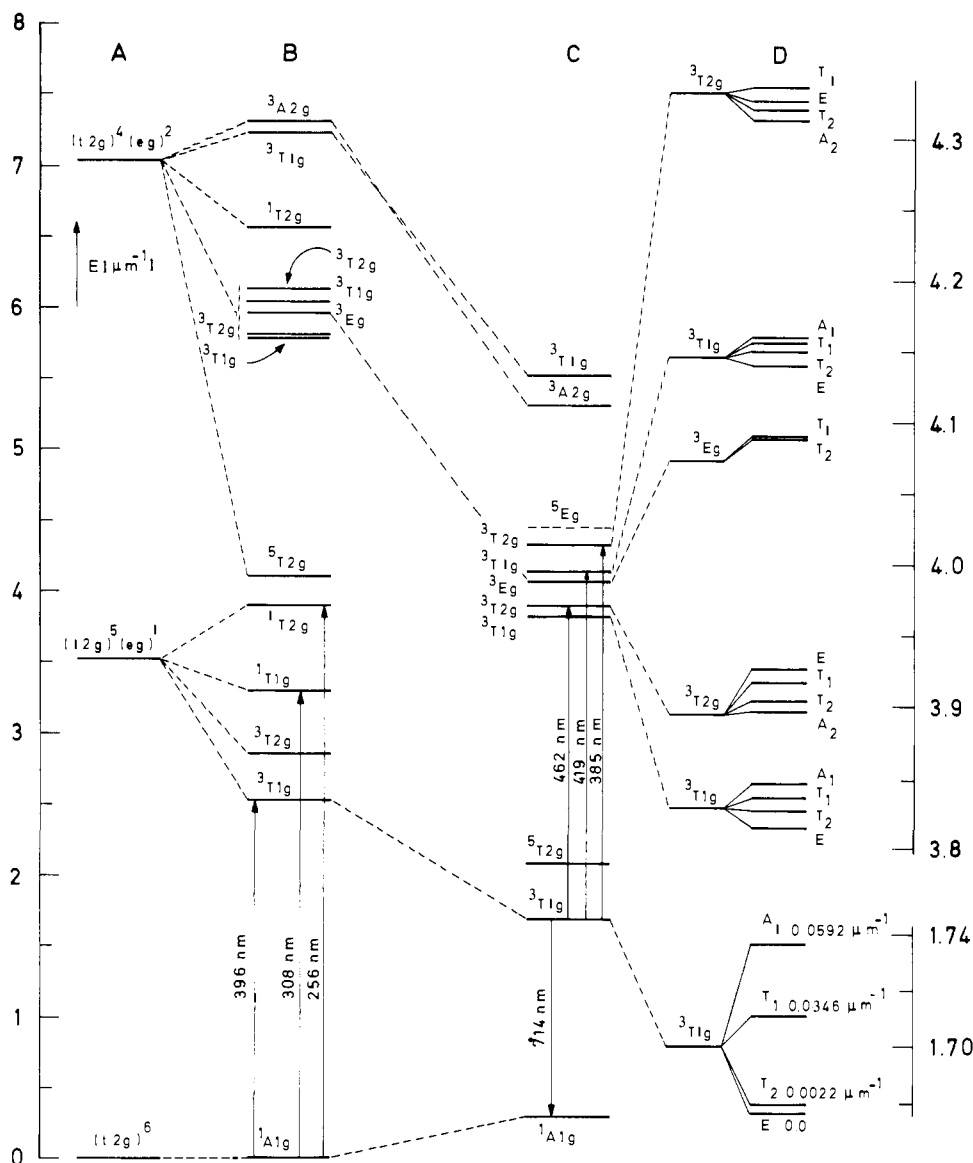


Figure 2. Calculated energy level diagram for $\text{Co}(\text{CN})_6^{3-}$: (A) parent configurations; (B) ligand field states based on ground-state geometry; (C) ligand field states based on ${}^3\text{T}_{1g}$ geometry; (D) effect of spin-orbit coupling (notice that the scale for t^5e^1 is twice as sensitive as for t^4e^2), $\zeta = 0.06 \mu\text{m}^{-1}$.

parentage) contain a common term $11C$ in the diagonal elements, while the remaining two triplets of this configuration (${}^3\text{A}_{2g}$ and one ${}^3\text{T}_{1g}$) contain a corresponding term of $14C$ and $13C$, respectively. Therefore the lower cluster is separated roughly by C or $2C$ from the higher levels, while the intra-cluster energy splittings are essentially modulated by the smaller B parameter. From Table I, it is clear that the energy range spanned by the lowest (five triplet) cluster will be $4B$ in first order; this range will be doubled to $\sim 8B$ or $0.35 \mu\text{m}^{-1}$ after matrix diagonalization.

2. Stokes Shift and Structural Relaxation. Excitation from the ${}^1\text{A}_{1g}$ ground state to the lowest ligand field ${}^3\text{T}_{1g}$ state corresponds to a $t_{2g} \rightarrow e_g$ transition. Owing to the σ -antibonding nature of the e_g orbitals, the ${}^3\text{T}_{1g}$ state will be characterized by an increased metal-ligand equilibrium distance. The long-lived triplet state will therefore relax toward a metastable level, corresponding to an expanded—but still octahedral²¹—coordination sphere (Figure 3). Obviously this relaxation process will be accompanied by a modification of the ligand field parameters.

In principle the parameter set (Dq, B, C) has to be replaced by a new set (Dq', B', C'). One anticipates Dq' to be smaller than Dq , while B' and C' might be slightly larger than B and

C (reduced covalency and reduced nephelauxetic effect).¹⁸ Therefore, in a correlation diagram, the energy level scheme should be expected to shift from the very strong field side toward a medium strong field.

A quantitative estimate of this effect can be obtained from the luminescence spectrum: a broad-band phosphorescence with a maximum at $\sim 1.4 \mu\text{m}^{-1}$ (714 nm) is observed in crystalline $\text{K}_3\text{Co}(\text{CN})_6$. The Stokes shift of the ${}^1\text{A}_{1g} \rightarrow {}^3\text{T}_{1g}$ absorption therefore amounts to $\sim 1.1 \mu\text{m}^{-1}$; this is a very large value indeed, but it is not untypical of strong-field d^6 complexes such as $\text{Rh}(\text{III})$ or $\text{Ir}(\text{III})$.¹² As shown in Figure 3, the luminescence and the absorption are both vertical processes; the emission wavelength reflects the ligand field parameters of a complex, where the metal-ligand equilibrium distance corresponds to the excited ${}^3\text{T}_{1g}$ state.

The ${}^1\text{A}_{1g} \rightarrow {}^3\text{T}_{1g}$ absorption energy of $\sim 2.5 \mu\text{m}^{-1}$ is given by $10Dq - 3C$; the ${}^3\text{T}_{1g} \rightarrow {}^1\text{A}_{1g}$ emission energy of $\sim 1.4 \mu\text{m}^{-1}$ is given by $10Dq' - 3C'$. Obviously, the change from C to C' can account for a shift of at most $\sim 0.1 \mu\text{m}^{-1}$ (the upper limit of C' being the free ion C_0 value of $\sim 0.4 \mu\text{m}^{-1}$). Therefore, nearly the complete Stokes shift should be due to a decrease of $10Dq$, and $10Dq'$ must be approximately $3.5 - 1.1 \sim 2.4 \mu\text{m}^{-1}$. The reduction is considerable but, as pointed out al-

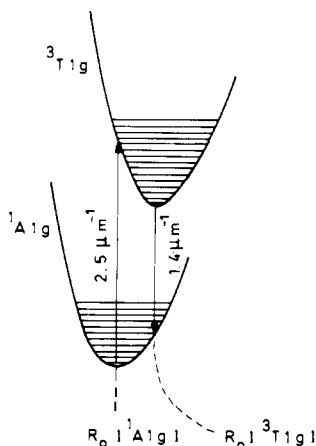


Figure 3. Relative position of the $^1A_{1g}$ and $^3T_{1g}$ potential energy surfaces.

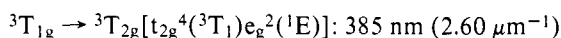
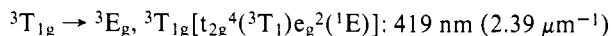
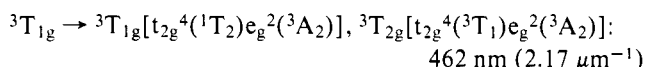
ready, the expanded molecule remains a strong field complex. Apart from a general closing up of the different configurations, the qualitative features of Figure 2B will remain valid. More specifically, the t^4e^2 configurations will remain characterized by a cluster of five triplets separated from another set of two triplets. Numerically, the energy range of the lower cluster may be expected to be $0.4\text{--}0.5 \mu\text{m}^{-1}$, and the upper cluster will be at least 0.7 or $0.8 \mu\text{m}^{-1}$ higher in energy.

Therefore, we assign the observed spectrum between 2.1 and $2.7 \mu\text{m}^{-1}$ to transitions between $^3T_{1g}$ and the first triplet cluster only. The transitions to the next two triplet states are expected at $3.5 \mu\text{m}^{-1}$ or higher. In that region, they will overlap with the ligand field transitions from the ground state, and will be difficult to observe. Therefore, a more precise estimate of C' appears to be impossible from the present results.

In order to proceed, it seems reasonable to put $C' = C$. Indeed, from the comparison of a number of different complexes, it has been found that C is much less sensitive to decreasing covalency than B . Moreover, the calculation of the first triplet cluster is particularly insensitive to the exact value of C' . An eventual more exact specification of C' (due to subsequent experimentation, for example) might be interesting in se, but will be without consequence for the present discussion.

In this way, an optimal fitting of the experimental spectrum is obtained with $C' = C = 0.3548 \mu\text{m}^{-1}$, $10Dq' = 2.37 \mu\text{m}^{-1}$, and $B' = 0.06 \mu\text{m}^{-1}$ (as compared to $B = 0.0448 \mu\text{m}^{-1}$). The 30% increase of B appears reasonable in the context of a decreasing nephelauxetic effect.

Figure 2C shows an energy level diagram calculated by means of this parameter set. The first triplet cluster separates more clearly into three distinct regions than in the unrelaxed molecule (Figure 2B). This is due on the one hand to the increased value of B' , and on the other hand to the increased interaction with the neighboring configurations. The level position quite obviously suggests the following assignments:



where the leading configurations are given in square brackets. It should also be stressed that the intensity distribution of the spectrum (two strong bands and one weak band) corresponds precisely to the number of triplet levels in the assignment.

In Figure 2C, the ground state $^1A_{1g}$ was arbitrarily set at $0.3 \mu\text{m}^{-1}$ above the ground state of Figure 2B. In this way, we indicate the vibrational excitation of the molecule resulting from a vertical phosphorescence.

Table II. Ω Coefficients and Reduced Matrix Elements of the Spin-Orbit Coupling Operator

3T_1		3T_2		3E	
components	Ω	components	Ω	components	Ω
A_1	$1/3$	A_2	$1/3$	T_1	0
T_1	$1/6$	T_2	$1/6$	T_2	0
T_2	$-1/6$	T_1	$-1/6$		
E	$-1/6$	E	$-1/6$		

$2S+1\Gamma$	reduced matrix element
$^3T_{1g}(t^5e^1)$	$3/2\zeta$
$^3T_{1g}[t_{2g}^4(^1T_2)e_g^2(^3A_2)]$	0
$^3T_{1g}[t_{2g}^4(^3T_1)e_g^2(^1E)]$	$3/2\zeta$
$^3T_{2g}[t_{2g}^4(^3T_1)e_g^2(^3A_2)]$	$-3/2\zeta$
$^3T_{2g}[t_{2g}^4(^3T_1)e_g^2(^1E)]$	$3/2\zeta$

3. Spin-Orbit Coupling. Hipps and Crosby¹⁰ deduced the spin-orbit splitting of the phosphorescent $^3T_{1g}$ state from the measurement of the lifetime as a function of temperature. They obtained a value of $\zeta(3d) \sim 0.06 \mu\text{m}^{-1}$. In principle, energy splittings of this order of magnitude might be able to blur the difference between the three regions that were predicted in the previous section. Therefore, it is necessary to investigate how spin-orbit coupling affects the energy levels. The results of a detailed numerical calculation (with $\zeta = 0.06 \mu\text{m}^{-1}$) are shown in Figure 2D. Two conclusions are immediately obvious.

(1) For $^3T_{1g}(t^5e^1)$, the results of Hipps and Crosby are confirmed: the four resulting levels are in the order and approximately at the positions found earlier.

(2) The spin-orbit splitting is much smaller for the t^4e^2 triplet cluster levels than in $^3T_{1g}(t^5e^1)$; the subdivision of the cluster into three separated regions remains unaffected.

These results can be rationalized in part by using the first-order expressions, derived from Griffith's irreducible tensor method.¹⁹ Let $2S+1\Gamma$ denote a given term as before, t one of the irreducible representations resulting from spin-orbit coupling, and τ one of its components. Then

$$\langle 2S+1\Gamma t \tau | \mathcal{H}_{\text{soc}} | 2S+1\Gamma t \tau \rangle = \Omega \begin{pmatrix} S & S & T_1 \\ \Gamma & \Gamma & t \end{pmatrix} \langle S, \Gamma || \mathcal{H}_{\text{soc}} || S, \Gamma \rangle$$

where the second factor at the right-hand side is the reduced matrix element, which is independent of t or τ . In Table II, the Ω coefficients and the reduced matrix elements are given explicitly for the relevant triplets.

The first-order energy splittings of $^3T_{1g}(t^5e^1)$ are given by $A_1(\zeta/2)$, $T_1(\zeta/4)$, T_2 , $E(-\zeta/4)$, corresponding to a global first-order range of $3/4 \zeta = 0.045 \mu\text{m}^{-1}$; the numerical result of Figure 2D ($0.0593 \mu\text{m}^{-1}$), as well as the splitting between E and T_2 , is due to complete configuration interaction.

Within the triplet cluster, two obvious factors tend to reduce the spin-orbit splitting. First, the Ω coefficients of 3E are zero. Second, the two zero-order $^3T_{1g}(t^4e^2)$ states are strongly mixed by the electron repulsion operator. One of them is characterized by a zero reduced matrix element; therefore, the total spread of neither of them is very large and amounts approximately to $(3/8)\zeta$.

Concluding Remarks. Relevance to Photochemistry

1. The calculation of the qualitative and the quantitative features of the excited-state spectrum strongly suggests that the absorbing species is the triplet $^3T_{1g}$, apparently relaxed along a totally symmetric relaxation coordinate.

2. It has been possible to derive, within certain limits, ligand field parameters characteristic for the excited molecule. As a consequence, the Co^{3+} intermediate-spin ($S = 1$) system could—for the first time—be studied in some detail.

3. The ³T_{1g} state is the photoactive state in a number of ligand substitution reactions. The qualitative features of these reactions have been described and rationalized in terms of the ligand field parameters of the original (ground state) molecule.²⁰ Since the actual parameters of the reacting entity apparently are rather different, one might be tempted to reject this attitude. We are inclined to believe that this is not necessary. Indeed, relaxation is the first step on the dissociative reaction path. By calculating the weakest bond in the initial complex (vertically above the ground state), one determines the most favorable reaction and relaxation coordinates; the course of the photochemical reaction is therefore correctly predicted on the basis of the ground-state parameters.

4. So far, it is not well understood why Co(NH₃)₆³⁺ and its derivatives are characterized by a much lower quantum yield for photosubstitution than Co(CN)₆³⁻ and its derivatives. A possible explanation is found from Figure 2. If a calculation as in Figure 2C is extrapolated for Co(NH₃)₆³⁺, the ⁵T_{2g} state drops below ³T_{1g} in the expanded molecule! A triplet–quintet crossover takes place in the course of the molecular relaxation. Most molecules follow the energetically favorable quintet path which may not have the properties required for photoreaction; hence the molecule can fall back to the ground state without reaction. Only a few molecules would follow the triplet path and be responsible for the observed quantum yield.

Acknowledgments. Two of the authors (L.V. and J.D.) are indebted to the F.K.F.O. (Fonds voor Kollektief Fundamenteel Onderzoek, Belgium) for financial support.

References and Notes

- (1) (a) Laboratory of Inorganic and Analytical Chemistry; (b) Laboratory of Quantum Chemistry.
- (2) Z. Stasicka and A. Marchaj, *Coord. Chem. Rev.*, **23**, 131–181 (1977).
- (3) R. A. Krause, I. Trabjerg, and C. J. Ballhausen, *Chem. Phys. Lett.*, **3**, 297 (1969).
- (4) T. Ohno and S. Kato, *Bull. Chem. Soc. Jpn.*, **43**, 8 (1970); **46**, 1602 (1973).
- (5) S. C. Pyke, M. Ogasawara, L. Kevan, and J. F. Endicott, *J. Phys. Chem.*, **82**, 302 (1978).
- (6) M. Maestri, F. Bolletta, L. Moggi, V. Balzani, M. S. Henry, and M. Z. Hoffman, *J. Am. Chem. Soc.*, **100**, 2694 (1978).
- (7) R. Benasson, C. Salet, and V. Balzani, *J. Am. Chem. Soc.*, **98**, 48 (1976).
- (8) A. W. Adamson, M. Larson, and R. Fukuda, results communicated at the VII IUPAC Symposium on Photochemistry, Leuven, July 1978.
- (9) M. Mingardi and G. B. Porter, *J. Chem. Phys.*, **44**, 4354 (1966).
- (10) K. W. Hipps and G. A. Crosby, *Inorg. Chem.*, **13**, 1543 (1974).
- (11) E. Zinato in "Concepts of Inorganic Photochemistry", A. W. Adamson and P. D. Fleischauer, Eds., Wiley-Interscience, New York, 1975, Chapter 4.
- (12) G. B. Porter in ref 11, Chapter 2.
- (13) Room temperature values in EPA solution are 314 and 260 nm, respectively. Upon cooling to the working temperature the first band shifts to about 308 nm. We assumed a similar UV shift for the second absorption.
- (14) J. Fujita and Y. Shimura, *Bull. Chem. Soc. Jpn.*, **36**, 128 (1963).
- (15) Barbara Loeb and F. Zuloaga, *J. Phys. Chem.*, **81**, 59 (1977).
- (16) The very weak absorption, reported in ref 9, at about 540 nm in the crystalline phase could not be observed.
- (17) J. S. Griffith, "The Theory of Transition-Metal Ions", Cambridge University Press, New York, 1971, Appendix 2, Table A29.
- (18) M. Gerloch and R. C. Slade, "Ligand Field Parameters", Cambridge University Press, New York, 1973.
- (19) J. S. Griffith, "The Irreducible Tensor Method for Molecular Symmetry Groups", Prentice-Hall, Englewood Cliffs, N.J., 1962.
- (20) L. G. Vanquickenborne and A. Ceulemans, *J. Am. Chem. Soc.*, **99**, 2208 (1977); **100**, 475 (1978).
- (21) K. W. Hipps, G. A. Merrell, G. A. Crosby, *J. Phys. Chem.*, **80**, 2232 (1976).

Intramolecular Hydrolysis of Glycinamide and Glycine Dipeptides Coordinated to Cobalt(III). 2. Reactions of the *cis*-[Co(en)₂(OH₂/OH)(glyNHR)]^{3+/2+} Ions (R = H, CH₂CO₂C₃H₇, CH₂CO₂⁻) and the Effect of Buffer Species

C. J. Boreham, D. A. Buckingham,*† and F. R. Keene†

Contribution from the Research School of Chemistry, Australian National University, Canberra, A.C.T., Australia 2600. Received April 19, 1978

Abstract: The intramolecular addition of cobalt(III) bound H₂O and OH⁻ to glycinamide, glycylglycine isopropyl ester, and glycylglycine also coordinated to Co(III) in the *cis*-[Co(en)₂(OH₂/OH)(glyNHR)]^{3+/2+} ions (R = H, CH₂CO₂C₃H₇, CH₂CO₂⁻) has been investigated both in the absence and presence of buffers. For the dipeptide complex (R = CH₂CO₂C₃H₇) both the aqua and hydroxo species form [Co(en)₂(glyO)]²⁺, but loss of hydroxide also occurs resulting in the chelated amide [Co(en)₂(glyNHR)]³⁺. A combination of rate and product analysis data suggests that the initial cyclization is rate determining under all conditions. Buffer species act as general bases in this rate-determining process, but they also enhance the formation of the hydrolysis product. Coordinated water is more reactive than coordinated hydroxide owing largely to a more positive ΔS[‡].

In this paper we compare the hydrolysis of glycinamide, glycylglycine, and glycylglycine isopropyl ester coordinated to Co(III) as monodentate ligands to the hydrolysis of the same substrates chelated to Co(III). In the former *cis*-[Co(en)₂(OH₂/OH)(glyNHR)]^{3+/2+} species the amide or dipeptide is attached to the metal through the amino group only, whereas in [Co(en)₂(glyNHR)]³⁺ the oxygen atom of the amide function is also coordinated. The two reactions are schemati-

cally represented by Schemes I and II (the oxygen atoms show the fate of hydroxide in the different situations).

¹⁸O-Tracer results have established that the coordinated oxygen atom in *cis*-[Co(en)₂(OH₂/OH)(glyNHR)]^{3+/2+} is retained in the hydrolyzed product [Co(en)₂(glyO)]²⁺, and that under alkaline conditions the [Co(en)₂(glyNHR)]³⁺ product also includes the label in the O-bound amide function.¹ These facts require hydrolysis of the monodentate and chelated amide systems **1** and **2** to be interconnected, and in this respect this study bears a close resemblance to the non-metal-catalyzed lactonization of 4-hydroxybutyramides^{2,3} and 2-hydroxy-methylbenzamides^{4,5} where direct intramolecular participation

† Department of Chemistry and Biochemistry, James Cook University of North Queensland, Townsville, Queensland, Australia 4811 (F.R.K.), and Department of Chemistry, University of Otago, P.O. Box 56, Dunedin, New Zealand (D.A.B.).